Titchener SA, Nayagam DAX, Kvansakul J, Kolic M, Baglin EK, Abbott CJ, McGuinness MB, Ayton LN, Luu CD, Greenstein S, Kentler WG, Shivdasani MN, Allen PJ, Petoe MA. A Second-Generation (44-Channel) Suprachoroidal Retinal Prosthesis: Long-Term Observation of the Electrode–Tissue Interface. *Trans Vis Sci Tech*. 2022;11(6):12.

doi: https://doi.org/10.1167/tvst.11.6.12

tvst

Article

A Second-Generation (44-Channel) Suprachoroidal Retinal Prosthesis: Long-Term Observation of the Electrode–Tissue Interface

Samuel A. Titchener[1,2], David A. X. Nayagam[1,3,4], Jessica Kvansakul[1,2], Maria Kolic[4], Elizabeth K. Baglin[4], Carla J. Abbott[4,5], Myra B. McGuinness[4,6], Lauren N. Ayton[4,5,7], Chi D. Luu[4,5], Steven Greenstein[1,8], William G. Kentler[8], Mohit N. Shivdasani[9,1], Penelope J. Allen[4,5], and Matthew A. Petoe[1,2]

[1] Bionics Institute, East Melbourne, Victoria, Australia
[2] Medical Bionics Department, University of Melbourne, Melbourne, Victoria, Australia
[3] Department of Pathology, University of Melbourne, Victoria, Australia
[4] Centre for Eye Research Australia, Royal Victorian Eye & Ear Hospital, Melbourne, Victoria, Australia
[5] Ophthalmology, Department of Surgery, University of Melbourne, Melbourne, Victoria, Australia
[6] Centre for Epidemiology and Biostatistics, Melbourne School of Population and Global Health, University of Melbourne, Melbourne, Victoria, Australia
[7] Department of Optometry and Vision Sciences, University of Melbourne, Melbourne, Victoria, Australia
[8] Department of Biomedical Engineering, University of Melbourne, Melbourne, Victoria, Australia
[9] Graduate School of Biomedical Engineering, University of New South Wales, Kensington, NSW, Australia

Correspondence: Matthew A. Petoe, Bionics Institute, 384-388 Albert St, East Melbourne 3002, Australia.
e-mail: mpetoe@bionicsinstitute.org

Received: December 13, 2021
Accepted: May 21, 2022
Published: June 13, 2022

Keywords: retinal implant; visual prosthesis; retinitis pigmentosa

Citation: Titchener SA, Nayagam DAX, Kvansakul J, Kolic M, Baglin EK, Abbott CJ, McGuinness MB, Ayton LN, Luu CD, Greenstein S, Kentler WG, Shivdasani MN, Allen PJ, Petoe MA. A second-generation (44-channel) suprachoroidal retinal prosthesis: Long-term observation of the electrode–tissue interface. Transl Vis Sci Technol. 2022;11(6):12, https://doi.org/10.1167/tvst.11.6.12

Purpose: To report the long-term observations of the electrode–tissue interface and perceptual stability in humans after chronic stimulation with a 44-channel suprachoroidal retinal implant.

Methods: Four subjects (S1–4) with end-stage retinitis pigmentosa received the implant unilaterally (NCT03406416). Electrode impedances, electrode–retina distance (measured using optical coherence tomography imaging), and perceptual thresholds were monitored up to 181 weeks after implantation as the subjects used the prosthesis in the laboratory and in daily life. Stimulation charge density was limited to 32 μC/cm^2 per phase.

Results: Electrode impedances were stable longitudinally. The electrode–retina distances increased after surgery and then stabilized, and were well-described by an asymptotic exponential model. The stabilization of electrode–retina distances was variable between subjects, stabilizing after 45 weeks for S1, 63 weeks for S2, and 24 weeks for S3 (linear regression; $P_{gradient} > 0.05$). For S4, a statistically significant increase in electrode–retina distance persisted ($P < 0.05$), but by the study end point the rate of increase was clinically insignificant (exponential model: 0.33 μm/wk). Perceptual electrical thresholds were stable in one subject, decreased over time in two subjects (linear model; $P < 0.05$), and increased slightly in one subject but remained within the predefined charge limits ($P = 0.02$).

Conclusions: Chronic stimulation with the suprachoroidal retinal prosthesis over 3 years resulted in stable impedances, small individual changes in perceptual electrical thresholds, and no clinically significant increase in electrode–retina distances after a period of settling after surgery.

Translational Relevance: Chronic stimulation with the 44-channel suprachoroidal retinal implant with a charge density of up to 32 μC/cm^2 per phase is suitable for long-term use in humans.

Introduction

Retinal prostheses can provide artificial vision to those with profound vision loss owing to retinal degenerative diseases such as retinitis pigmentosa.[1–3] This goal is achieved by electrically stimulating the retina using implanted electrodes to evoke artificial percepts, termed phosphenes. For optimal outcomes, phosphenes should be reproducible—the response of the retina to an arbitrary stimulation sequence should remain stable over time.

One factor that can affect evoked responses and their reproducibility is the electrode–tissue interface, which modifies how charge is transferred from the electrode into the surrounding tissue, and ultimately determines perceptual thresholds.[4] The electrode–tissue interface is the result of complex interplay of many factors, including cellular and physiological factors that are difficult to observe in vivo. The distance from the electrode to the retina is one factor that is readily observable in living subjects via optical coherence tomography (OCT) imaging. The electrical impedance of the electrode is also readily measurable and is sensitive to changes in the electrode–tissue interface.[5]

The interplay between perceptual thresholds, electrode–retina distance, and impedance has been described in previous studies. Perceptual thresholds have been reported to increase with electrode–retina distance in epiretinal implant recipients[6–9] and suprachoroidal retinal implant recipients.[10] This increase happens because the target neurons are further from the concentrated electrical fields near the electrode when the electrode–retina distance is great. Electrode impedance has also been shown to be correlated with perceptual thresholds and inversely correlated with the electrode–retina distance and can also be affected by the presence of fluid and fibrotic tissue, which can potentially increase during inflammation.[6–10] Inflammation can occur in tissue surrounding implants and may potentially be exacerbated owing to chronic electrical stimulation. Furthermore, these relationships may be confounded by variables such as the location of the electrode on the retina (with respect to the fovea) and the severity of retinal degeneration in the vicinity of specific electrodes.

A prototype suprachoroidal retinal implant was trialed by our group between 2012 and 2014 (NCT01603576). Phosphenes were elicited reliably in a laboratory environment, and the device provided improvement in visual function tasks.[11,12] Despite the general success of the prototype, we observed that perceptual thresholds increased over the course of the study, accompanied by steadily increasing electrode–retina distances.[10] It was hypothesized that electrical stimulation with the implant triggered an inflammatory response or increased the thickness of the fibrotic capsule, causing the electrode–retina distance to increase. This hypothesis in turn led to a compounding effect of increased perceptual thresholds, requiring even higher levels of stimulation, leading to further inflammation or fibrosis. Perceptual thresholds remained within the stimulator's compliance for the 24-month study period, after which the study protocol mandated explantation of the percutaneous connector. Nevertheless, there was concern that perceptual thresholds may have eventually increased to a point that it was no longer possible to reliably elicit phosphenes, had the study continued for longer.

The development of a second-generation fully implantable suprachoroidal retinal prosthesis prompted further preclinical investigation to more accurately determine tolerable levels of chronic stimulation.[13–15] On the basis of these studies, the safe charge density limits were revised from 237 $\mu C/cm^2$ in the prototype trial to 32 $\mu C/cm^2$. This difference was achieved by increasing the electrode diameter (now ø1 mm compared with 0.6 mm and 0.4 mm) and decreasing the maximum allowable charge per phase. The maximum stimulation rate was also decreased from 400 to 50 pulses per second. It is expected that electrode–retina distances and perceptual thresholds will remain stable when stimulation is limited within these parameters.

A clinical trial of the second-generation suprachoroidal retinal prosthesis commenced in February 2018 (NCT03406416). Four participants were implanted with the prosthesis and used it both in the laboratory and unsupervised in their daily lives. Stimulation was within the revised charge density limits defined elsewhere in this article. All four subjects perceived phosphenes in response to electrical stimulation with the implant, and the prosthesis provided functional vision improvements and meaningful assistance in activities of daily living.[16–18] For these practical benefits to be sustained in the long term, it is important that chronic stimulation with the implant does not lead to a loss of device functionality owing to changes in the electrode–tissue interface.

The present study reports long-term observations of the electrode-tissue interface in four human subjects implanted with the second-generation suprachoroidal retinal prosthesis. Electrode–retina distance, electrode impedance, and perceptual threshold measurements were collected over approximately 3 years. We aim to assess the stability of perception and the electrode–tissue interface to determine whether chronic

stimulation within the pre-established limits leads to any adverse physiological reactions or impacts the long-term device usability.

Methods

Participants

This study presents data from four adult human subjects (S1–S4) who participated in the clinical trial of a 44-channel suprachoroidal retinal implant (NCT03406416) between 2018 and 2021.[16–18] The subjects were profoundly blind (bare light perception only) from end-stage retinitis pigmentosa and had the suprachoroidal retinal prosthesis implanted unilaterally in 2018 (Table 1). Device fitting commenced 8 weeks postoperatively, followed by training in laboratory and real-world environments and a minimum of 2 years of regular outcome measure assessments.[16–18] During this time the subjects used the prosthesis unsupervised in their daily lives and regularly visited the laboratory for training, functional vision assessment, and OCT imaging. Table 1 summarizes the subject demographics and the length of observation for each subject. Owing to the coronavirus disease 2019 (COVID-19) pandemic, there were differences in the timing of the study end point between subjects. The study was approved by the Royal Victorian Eye and Ear Hospital Human Research and Ethics Committee and was carried out in accordance with the tenets of the Declaration of Helsinki with the informed consent of all participants.

Suprachoroidal Retinal Prosthesis

The implantable components of the prosthesis comprise an array of 44 platinum disk electrodes (ø 1 mm) embedded in silicone, implanted in the suprachoroidal space, connected via subcutaneous cabling to two implanted stimulator units embedded in the skull behind the ear.[16] The surgical procedure is fully described in previous publications from our group.[11,19] Infrared fundus imaging showing the array position for subject S3 is displayed in Figure 1, with the electrodes visible as bright circles in the image, beneath the semitranslucent retina. Implant locations for all participants are shown in Supplementary Figure S1. Visual input to the system is provided by a camera mounted on a pair of spectacles. Images from the camera are processed by an externally worn portable vision processing unit, which then delivers stimulation commands to the implanted stimulators wirelessly through mutually coupled coils.[16] The stimulating electrodes were divided equally between the two implanted stimulator units, such that each stimulator could drive 22 of the 44 electrodes.

Stimulation Parameters

Electrodes were stimulated with charge-balanced biphasic pulse waveforms with 500 µs phase width, 500 µs interphase gap, and 1700 µs shorting period. Stimulation was limited to a maximum of 250 nC/phase and 50 pulses per second on the basis of results from preclinical chronic stimulation studies.[14,15] The device-fitting process determined the stimulation parameters to be deployed to the prosthesis. This process involved identifying the subset of electrodes that yielded useful phosphenes and setting the operational range of current levels for those electrodes. The remaining electrodes were inactive during normal operation of the device and only received stimulation during impedance measurements and occasional laboratory investigations. Inactive electrodes also received residual charge recovery current during the shorting period between pulses. In some cases, when

Table 1. Subject Demographics

Sex	S1 Male	S2 Male	S3 Female	S4 Male
Age at baseline (years)	47	63	66	39
Eye condition	RP (rod cone dystrophy)	RP (rod cone dystrophy)	RP (cone rod dystrophy)	RP (cone rod dystrophy)
Visual acuity	Light perception OU	Light perception OU	Light perception OU	Light perception OU
Age when legally blind (years)	20	34	41	13
Years of useful form vision	34	43	56	19
Implanted eye	Left	Right	Right	Right
Study end point (weeks postoperative)	154	156	178	181

OU, both eyes; RP, retinitis pigmentosa.

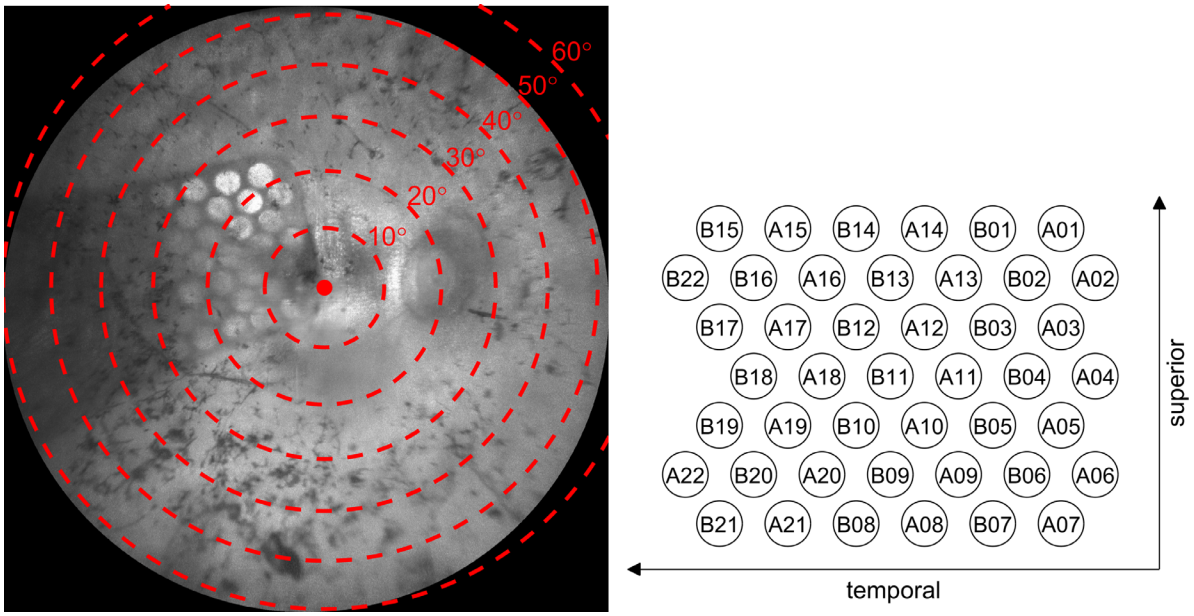

Figure 1. Position of electrodes relative to the fovea in subject S3. (*Left*) Infrared fundus imaging showing the location of the stimulating electrodes (visible as *bright circles*) and the silicone substrate (*dark shadow*) behind the retina. Concentric circles indicate degrees of visual field relative to the fovea (*red dot*) according to the Drasdo and Fowler schematic eye.[20,21] (*Right*) Electrode naming convention for a right eye implant. Electrode A06 in the inferior–nasal region is closest to the fovea for this subject (S3). The left eye implant is identical but mirrored horizontally. A and B refer to the stimulator unit that controlled that particular electrode (22 electrodes per stimulator).

a percept could not be reliably evoked within the 250 nC/phase limit, two neighboring electrodes were operated in a paired configuration to increase the effective surface area of the electrode–tissue interface, allowing up to 500 nC/phase. If the paired electrodes were associated with the same stimulator, then they were operated as a shorted pair, and if they were each associated with different stimulators, then they were synchronously stimulated.

In some cases, an electrode that reliably yielded a phosphene was nevertheless excluded in the deployed stimulation parameters. This occurred when the phosphene was confusing, indistinct, or interfered with the detection or interpretation of other phosphenes. For example, two neighboring electrodes may produce phosphenes that overlap significantly within the visual field, resulting in redundant visual information and a confusing percept. This outcome was most common for electrodes in eccentric locations.

Impedance Measurement

Electrode impedances were monitored longitudinally for all functional electrodes. Impedance was measured via telemetry by stimulating an electrode with a biphasic pulse waveform (75 µA, 500 µs phase width, 20 µs interphase gap), measuring the voltage across the current source at the end of the first phase using inbuilt instrumentation in the implanted stimulator, and dividing the measured voltage by the stimulation current. These stimulation parameters were kept consistent for all impedance measurements reported in this study, because the current and phase width can affect the measured impedance. The remaining electrodes were shorted together as a common-mode return. When subjects visited the laboratory for fitting, training, or outcome assessments, electrode impedances were always measured at the beginning of the session, before any other stimulation as well as at the conclusion of the session. When a subject used their prosthesis in daily life outside of the laboratory, impedances were measured only once, when the device was first powered up each day (before any other stimulation).

Monitoring Electrode Locations

The distance of the electrode from the retina was measured by manual inspection of OCT imaging, which was monitored over time (Spectralis, Heidelberg Engineering GmbH, Heidelberg, Germany).[16] Single section b-scans were taken through each electrode, revealing the location of the electrode with respect to the retinal layers. The inbuilt markup tools within the Heidelberg Spectralis Heyex software were then used to measure the distance from the center of the electrode

to the inner boundary of the retinal pigment epithelium. If an electrode was tilted relative to the retina, the distance was measured along the axis perpendicular to the electrode surface. The manual measurement was performed by three researchers who had training in performing electrode–retina distance measurements according to an internal standard operating procedure. Our previous study using a subset of these data showed excellent interobserver reliability using this method.[22] When the electrode–retina distance was able to be measured in multiple scans for any given electrode, the average distance is presented. Data are not available for all electrodes at all timepoints because it was not always possible to acquire clear images of the whole array. OCT imaging was collected every 1 to 2 weeks until approximately 24 weeks after surgery, after which imaging was less frequent (approximately every 12 weeks, subject to COVID-19 pandemic restrictions and the availability of the subjects).

The retinotopic location of each electrode with respect to the fovea was estimated from near infrared fundus imaging (Clarus 500, Zeiss; Spectralis, Heidelberg Engineering). The location of the fovea was determined by an experienced clinician using all available imaging modalities, and the location of the center of each electrode relative to the fovea was measured in mm, and then converted to degrees of visual field according to the Drasdo–Fowler schematic eye (Fig. 1).[20,21]

Perceptual Thresholds

Perceptual thresholds were measured using a two-down one-up modified staircase procedure described in a previous publication from our group.[10] In brief, participants were asked to respond yes whenever they saw a phosphene (presented as 0.5-second pulse trains at random intervals). The stimulus intensity began at 25 nC and was increased after each interval with a no or absent response, and decreased after intervals with two yes responses in succession. Each procedure ended after five turning points and the threshold was estimated as the average stimulus intensity of the last three turning points. The step size used to increase or decrease the charge during the staircase procedure was 1 dB (approximately 12%) until the first turning point and 0.33 dB (approximately 4%) thereafter. Because the threshold procedure was time consuming and fatiguing for the subjects, a subset of five electrodes (or pairs of electrodes) were selected for longitudinal monitoring in each subject. The electrodes were chosen to include a selection of subfoveal and peripheral electrodes. If the staircase procedure reached a charge of 250 nC per phase (or 500 nC per phase for paired electrodes) then the procedure was aborted and no threshold was recorded.

Statistical Methods

Nonlinear regression was used to model the change in electrode-retina distance over time using the function:

$$d(t) = b_0 + b_1 e^{-b_2 t},$$

where $d(t)$ is the electrode–retina distance (in microns) at time t (weeks from surgery), b_0 is the asymptote, b_1 is a scale factor, and b_2 is the time constant. Models were created separately for each subject and observations were clustered by electrode. To determine the point at which electrode–retina distances stabilized, a mixed effects linear model with random slopes and intercepts per electrode was fitted to all data for each subject separately. Data were iteratively excluded from the model, starting with the earliest measurements and advancing by date, until the slope of the linear model was not significantly different from zero (95% confidence interval contains zero). The relationship between impedance and the electrode–retina distance was investigated using a mixed effects linear model clustered by electrode fitted to the data for each patient. The relationships between perceptual thresholds and time, electrode–retina distance, and electrode eccentricity from the fovea, were tested using ordinary least-squares linear regression.

Results

Device Use

Device logs indicated that the frequency of unsupervised use for subjects S1 to S3 was every 6 to 7 days on average, for 2.3 ± 1.8 hours each instance. Subject S4 used the device on seven occasions for a maximum of half an hour each instance. The primary use case was for excursions outside of the home, and hence device usage was considerably decreased during COVID-19 pandemic restrictions. Device use statistics up to 56 weeks after implantation have been reported previously for this cohort.[16] The total charge delivered during the 2018 to 2021 study period was 7.71 C for S1, 4.19 C for S2, 18.45 C for S3, and 0.68 C for S4. Subject S4 had limited participation in the clinical trial owing to reasons unrelated to the study. The charge delivered per electrode per day is presented in Supplementary Figures 3, 5, 7, and 9.

Electrode–Retina Distances

Longitudinal electrode–retina distance measures are presented for each subject in Figure 2. Fitted parameters for the exponential model of the electrode–retina distance are presented in Table 2. Plots of the electrode–retina distance for each electrode individually are available in Supplementary Figures S2, S4, S6, and S8. For each subject, the electrode-to-retina distance against time is well-described by an asymptotic exponential fit (Fig. 2, black line), suggestive of an initial period of increasing distances immediately after

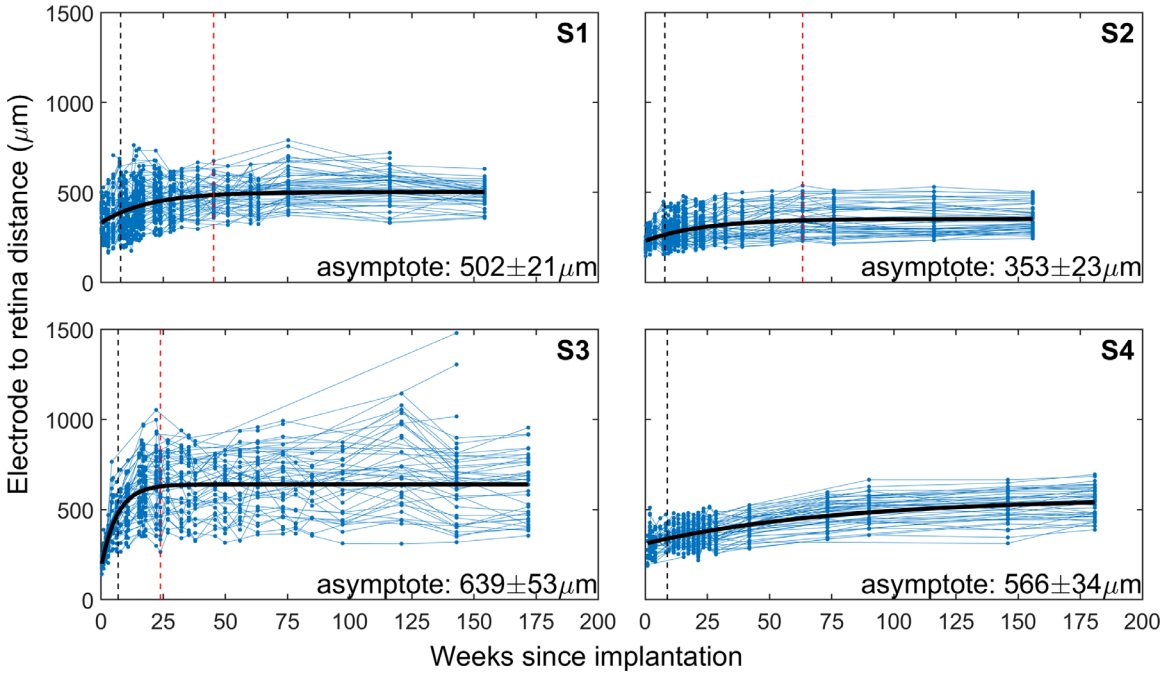

Figure 2. Longitudinal electrode–retina distance measures for all 44 stimulating electrodes for subjects S1 to S4. Data from all electrodes are included, but not all electrodes are represented at every time point. An asymptotic exponential model was fitted to the data (*solid black line*), suggesting an initial period of increasing distances that then settled to a stable value that was maintained for the rest of the study. The dashed black line indicates the switch-on date for each subject. There was no significant change in the average electrode-retina distance after 51 weeks postoperative for S1, 63 weeks postoperative for S2, and 17 weeks postoperative for S3, indicated by *dashed red lines* (linear model, $P_{gradient} > 0.05$). For S4, the electrode–retina distances continued to increase for the duration of the study, but seem to be approaching an asymptote.

Table 2. Fitted Parameters for Increasing Electrode–Retina Distance Over Time

Participant	Parameter[a]	Coefficient	95% CI	*P* Value
S1	b_0	501.9	[480.6 to 523.1]	<0.001
	b_1	−171.2	[−198.9 to −143.5]	<0.001
	b_2	0.0516	[0.0394 to 0.0641]	<0.001
S2	b_0	352.8	[329.5 to 376.1]	<0.001
	b_1	−122.1	[−143.2 to −101.0]	<0.001
	b_2	0.0417	[0.0323 to 0.0511]	<0.001
S3	b_0	638.6	[585.9 to 691.3]	<0.001
	b_1	−460.4	[−523.5 to −397.2]	<0.001
	b_2	0.1554	[0.1309 to 0.1804]	<0.001
S4	b_0	566.2	[532.6 to 599.9]	<0.001
	b_1	−255.0	[−278.7 to −231.3]	<0.001
	b_2	0.0126	[0.0078 to 0.0173]	<0.001

[a]Fitted to the model $d(t) = b_0 + b_1 e^{-b_2 t}$, where $d(t)$ is the electrode–retina distance at time t, b_0 is the asymptote, $(b_0 + b_1)$ estimates the average ER distance at day 0, and b_2 is a time constant.

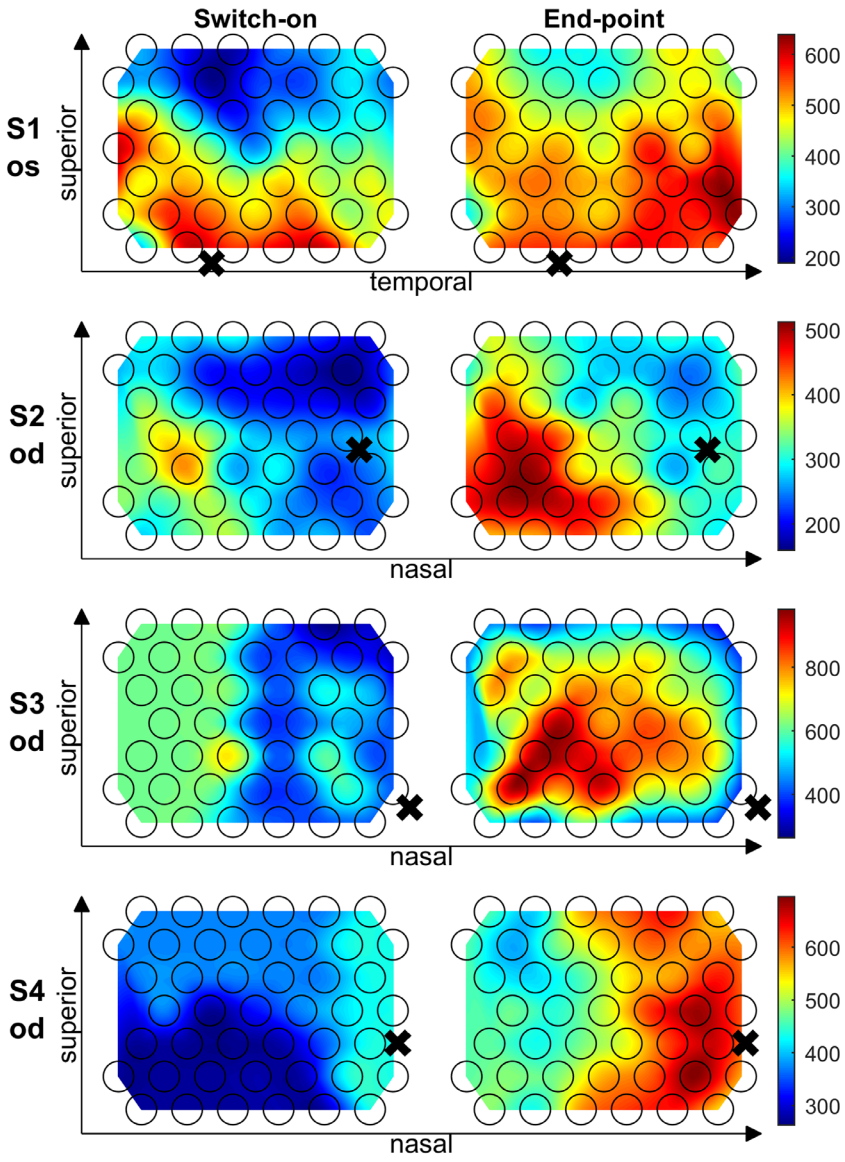

Figure 3. Heat maps showing electrode-retina distances across the electrode array for each subject (S1–S4) at device switch-on (left column) and at the study end point (*right column*). Color represents electrode to retina distance in microns. *Black circles* indicate electrode locations. A *black cross* marks the approximate location of the fovea for each subject. S1 received the implant in the left eye, and S2 to S4 received the implant in the right eye.

implantation, which then settled to a stable distance that was maintained for the rest of the study. There was no significant change in the electrode–retina distance after 45 weeks postoperative for S1, 63 weeks postoperative for S2, and 24 weeks postoperative for S3. For S4, a statistically significant increase in electrode-retina distance continued for the duration of the study (181 weeks), but the rate of increase slowed with time and the distance seems to be approaching an asymptote. At the study end point, the rate of increase in the electrode–retina distance for S4 was just 0.33 microns per week (nonlinear model). This analysis is limited by the sparsity of data after 43 days postoperative for S4, which is due to limited engagement in the study by this participant (for reasons not related to the study).

The variation in the electrode–retina distance across the electrode array is visualized in Figure 3, which shows measurements from the switch-on date (approximately 8 weeks postoperative) and the study end point (S1, 154 weeks; S2, 156 weeks; S3, 178 weeks; S4, 181 weeks). The distance from the retina is represented by color. The electrode–retina distances increased between switch-on and end point for all subjects. For

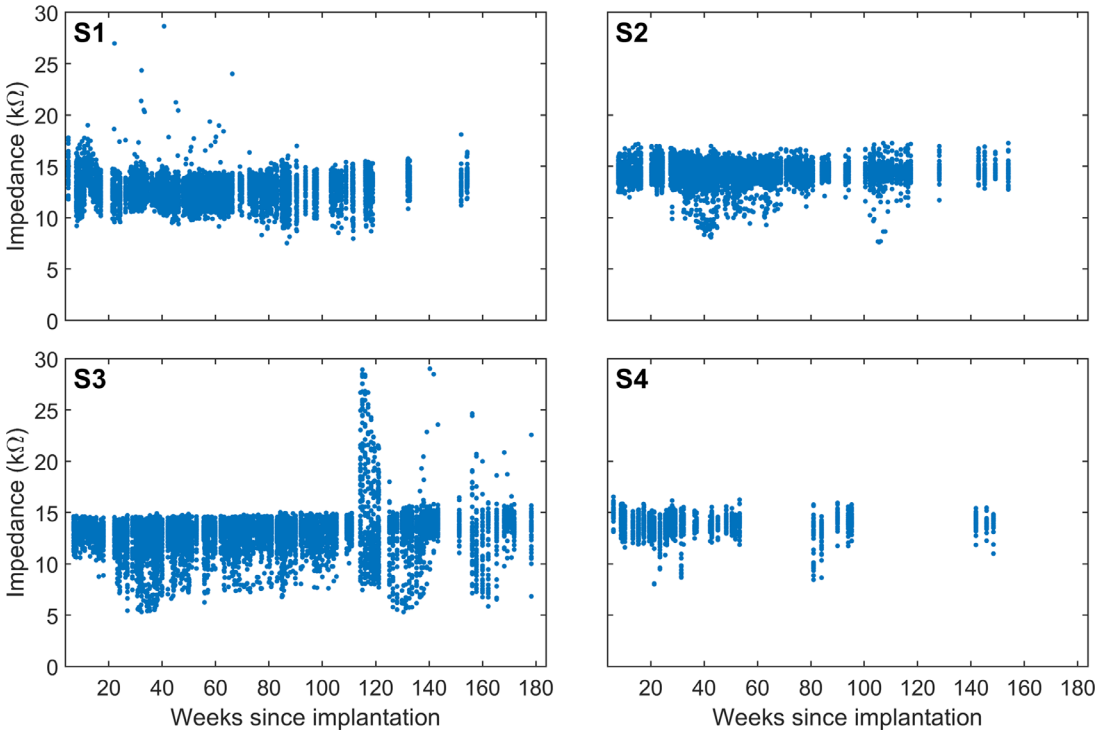

Figure 4. Longitudinal impedance measures for subjects S1 to S4, showing only impedances measured before any other stimulation each day.

S1 and S4, electrodes near the fovea were further from the retina than eccentric electrodes, whereas for S2 and S3, the electrodes near the fovea were generally closer to the retina.

Impedances

Four electrodes in total failed (open circuit) within 8 weeks after surgery; one for S1, two for S2, and one for S4. Impedance data from failed electrodes were not analyzed. Figure 4 displays the longitudinal electrode impedance measures for each subject, showing only impedance measurements before any stimulation each day. All subjects experienced some volatility in impedance in the initial weeks after surgery, before settling to a stable range of 10 to 16 kΩ for the remainder of the study. For S2 and S3, certain electrodes experienced transient high or low impedances, which are visible as outliers in Figure 4. These findings are examined in further detail elsewhere in this article. Impedance is plotted against electrode–retina distance in Figure 5, where each electrode–retina distance measurement is paired with an impedance measurement from the same date, demonstrating that impedances decreased with electrode–retina distance (mixed effects linear model, $P < 0.001$).

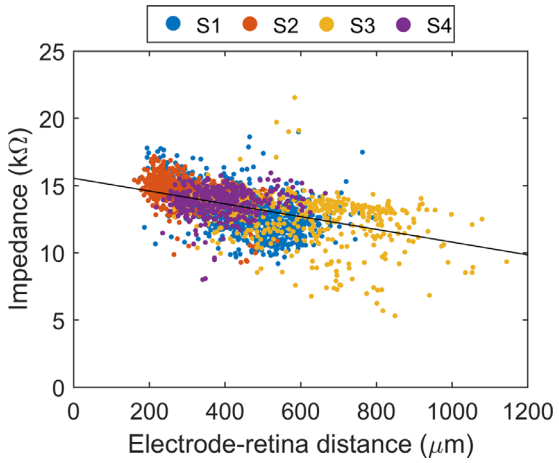

Figure 5. Impedance decreased with increasing electrode-retina distance. The black line represents a mixed-effects linear model fitted to impedance versus electrode-retina distance with subject as a random variable ($P < 0.001$).

Perceptual Thresholds

Although electrode combinations were not tested exhaustively, stimulation within the predefined charge density limit yielded phosphenes for 27 of 44 electrodes (61.4%) for S1, 32 (72.7%) for S2, 24 (54.5%) for S3, and 25 (56.8%) for S4, comprising predominantly foveal electrodes with sparser density at the periphery.

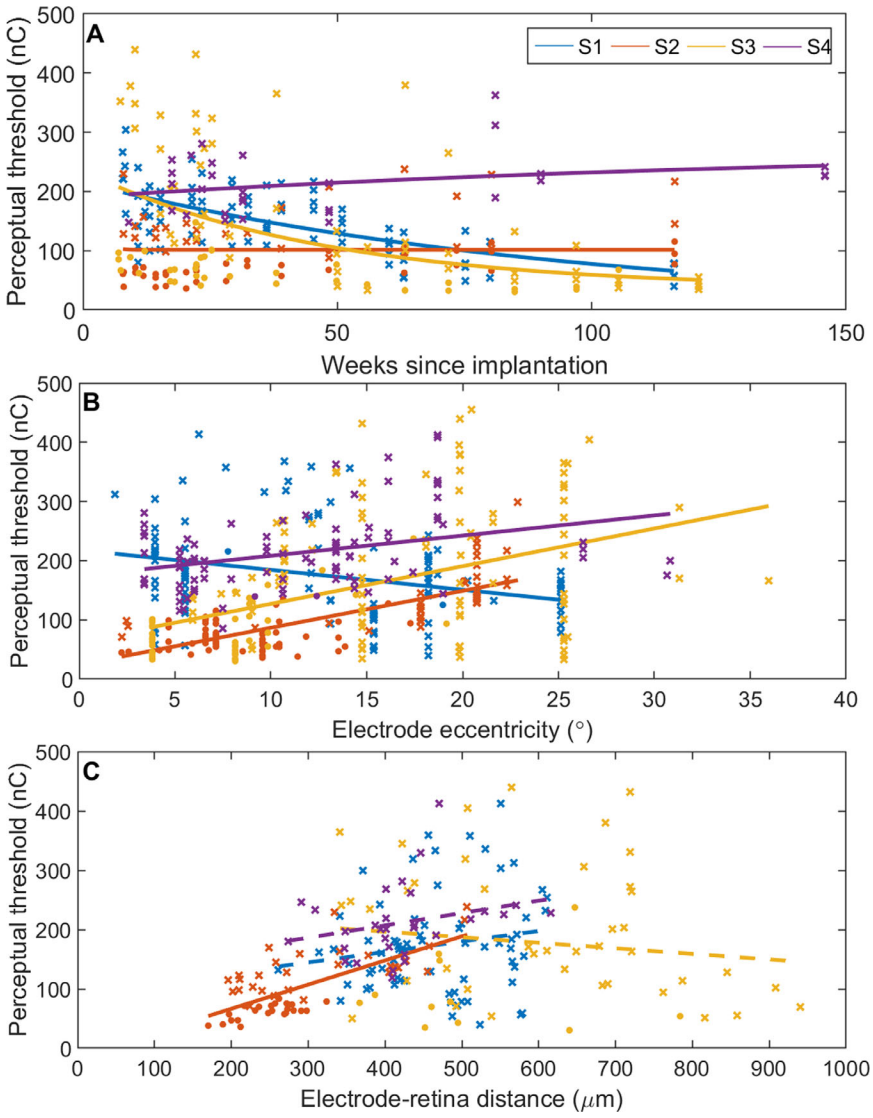

Figure 6. Perceptual thresholds for a subset of five electrodes per subject. *Circles* represent single electrodes, and *crosses* represent electrodes that were operated as synchronous or shorted pairs, which were typically used in peripheral locations where higher charge levels were required. Regression models fitted to the data are represented by *solid lines* when the gradient was significantly different from zero ($P < 0.05$) and *dashed lines* otherwise. (A) Perceptual thresholds and exponential fit over time. (B) Perceptual thresholds and linear fit against electrode eccentricity from the fovea. For shorted/synchronous pairs, the eccentricity was calculated from the centroid of the two electrodes. (C) Perceptual thresholds and linear fit against electrode–retina distance. For shorted/synchronous pairs, the average distance for the two electrodes is shown.

Note that not all electrodes that yielded a phosphene were included in the stimulus configuration that was deployed to the subject's device.

Perceptual thresholds for the subset of electrodes (or pairs of electrodes) that were selected for longitudinal monitoring are plotted against time in Figure 6A. Exponential regression models are fitted to the data for each subject. Thresholds decreased over time for S1 (−1.35 nC/week, $P < 0.001$) and for S3 (−1.40 nC/week, $P < 0.001$), suggesting familiarization with the phosphenes over time. Thresholds increased slightly over time for S2 (0.43 nC/week, $P = 0.021$), and there was no significant change in thresholds over time for S4 ($P = 0.13$). Thresholds increased with eccentricity from the fovea in S2, S3, and S4, but decreased with eccentricity in S1. This difference might be because the electrode–retina distances were greatest along the foveal edge of the array for S1 (Fig. 3). A significant correlation between perceptual thresholds and electrode–retina distances was observed only for S2 (0.41 nC/μm, $P < 0.001$). Perceptual thresholds remained measurable for all of the

tracked electrodes, and were sufficient to allow at least 2 dB of dynamic range within the predefined charge limits.

Transient Decrease in Impedance With Charge

Stimulation was associated with a short-term decrease in the impedance of the stimulated electrode. Figure 7 shows the percentage change in impedance over each day of stimulation, measured from the first impedance measurement of each day (before any stimulation) to the final impedance measurement of the day (after all other stimulation). The total charge delivered to the electrode over the day is plotted on the horizontal axis, which is scaled logarithmically. When electrodes were stimulated as a shorted pair, it is assumed that each electrode received one-half of the total charge delivered. Data are excluded from days on which the only stimulation that occurred was for the purpose of measuring impedance. Data are only included from days on which the prosthesis was used exclusively in the laboratory to ensure no stimulation occurred before the initial impedance test or after the final test. A logarithmic model was fitted to the data (Fig. 7, *black line*; $P < 0.001$ for all subjects). Impedance began to decrease after approximately 0.01 mC of charge was delivered, equal to forty pulses at 250 nC per phase, and the greatest change recorded was –68%.

Stimulus-related Changes in Impedance

Although impedances were generally stable longitudinally, a small number of electrodes experienced transient changes in impedance that correlated with periods of increased stimulation. Two such examples are presented in Figure 8. Figure 8A displays longitudinal impedance measures for S2 for electrodes A20 and B20, which have neighboring positions in the electrode array. Impedance for these two electrodes decreased temporarily significantly between approximately 30 and 70 weeks postoperatively, reaching a low of approximately 8 kΩ at 41 weeks postoperatively, down from approximately 14 kΩ (Fig. 8A). The onset and offset of the local minima corresponded very closely to a period of increased stimulation for these electrodes (Fig. 8C), and the peak in stimulation levels approximately coincided with the lowest impedance measurement. As stimulation levels subsided, impedance gradually returned to its initial value of approximately 14 kΩ. This activity did not seem to affect the electrode–retina distance for these electrodes, which maintained a slow increase that had begun before the period of increased stimulation levels (Fig. 8B). Impedances of the electrodes

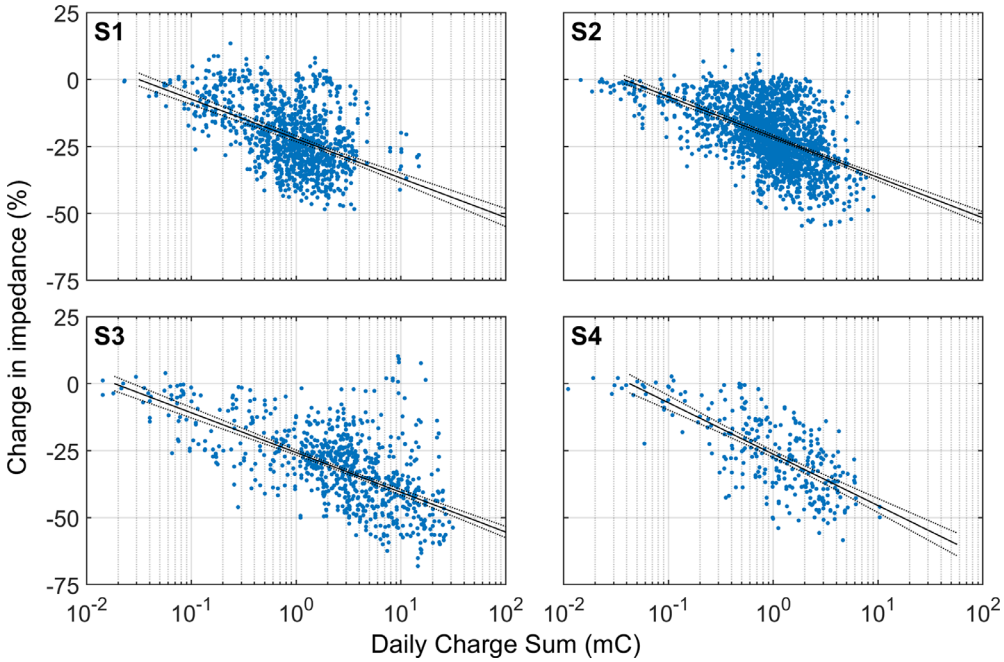

Figure 7. Impedance of electrodes decreased temporarily as they received stimulation. Changes in impedance from the start of each day to the end of each day for individual electrodes are plotted against the total charge delivered to the electrode over the course of the day. Data are excluded if the only stimulation delivered to an electrode was for impedance measurement. Note that the horizontal axis is logarithmic. A logarithmic function was fitted for each subject, represented by *black lines*, and the 95% CI indicated by *gray lines*.

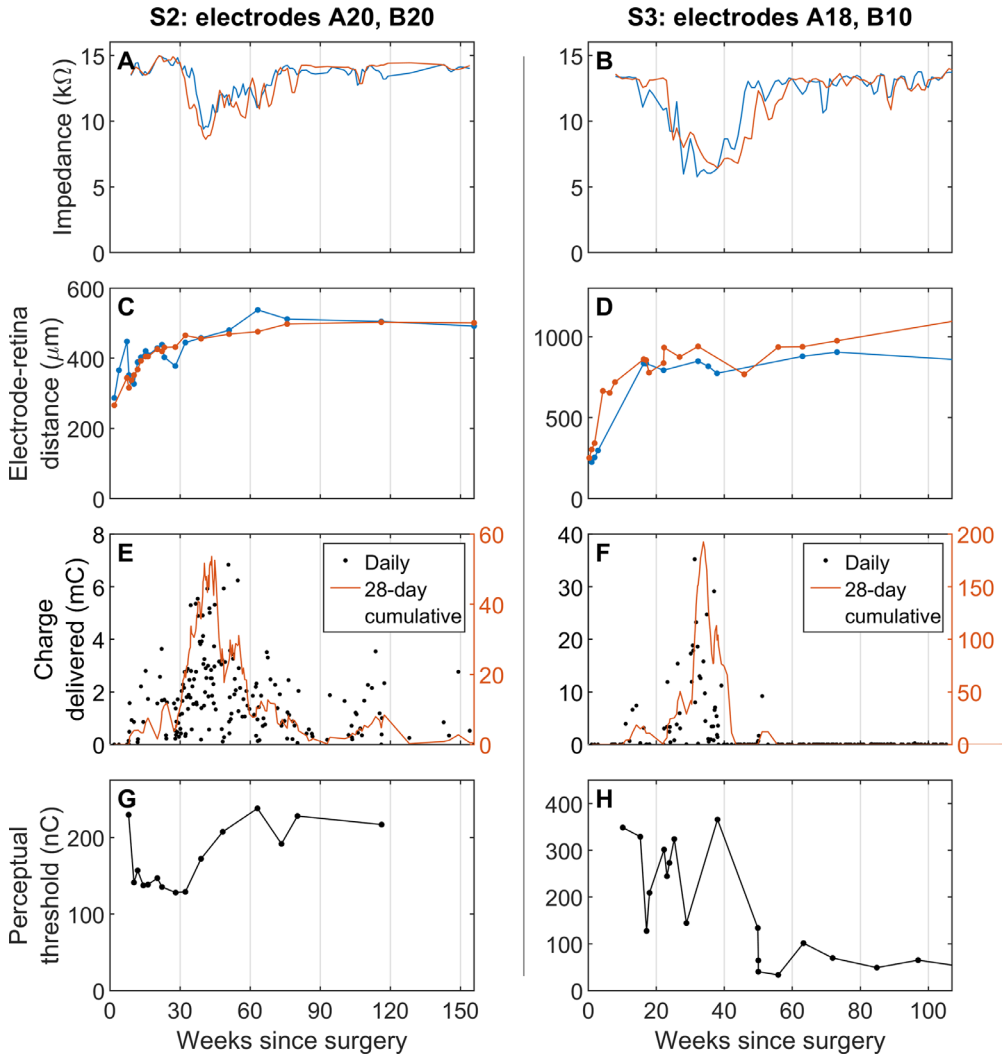

Figure 8. Stimulus-related changes in impedance were observed for a small number of electrodes. (A) Longitudinal impedance measures for S2 for electrodes A20 (*blue*) and B20 (*red*). (B) Electrode–retina distance for S2 electrodes A20 and B20. (C) Daily charge delivered to S2 electrodes A20 and B20. (D) Longitudinal perceptual threshold measures for S2 electrodes A20 and B20 (operated as a pair). (E) Longitudinal impedance measures for S3 A18 (*blue*) and B10 (*red*). (F) Electrode–retina distance for S3 electrodes A18 and B10. (G) Daily charge delivered to S3 electrodes A18 and B10. (H) Longitudinal perceptual threshold measures for S3 electrodes A18 and B10 (operated as a pair). Note that the vertical scales differ between subjects. Only impedance measures taken at the start of each day (before any other stimulation) are included. Impedance is smoothed using a median filter with a window width of 14 days. In both cases, the two electrodes occupy neighboring positions on the electrode array and were operated as a shorted pair, so the charge delivered to each electrode is the same.

adjacent to A20 and B20 were unaffected. Similar observations were made for S3 for electrodes A18 and B10, which also neighbor each other on the array, and are presented in Figure 8E through H; a temporary decrease in impedance occurred between 20 and 50 weeks postoperatively, coinciding with a period of increased levels of stimulation, and electrode–retina distances were not obviously affected.

Passive Changes in Impedance

Transient changes in impedances that were apparently unrelated to stimulation were observed over a large area of the array in one of the subjects (S3) between 115 and 140 weeks postoperatively. Figure 9 displays longitudinal impedances and electrode–retina distances for two groups of electrodes: a cluster of electrodes near the temporal edge of the array (*blue*) and a group of electrodes along the superior and inferior edges of the array (*red*). A sudden spike in impedance was observed at approximately 114 weeks postoperatively in both groups of electrodes as shown in Figure 9. This spike was immediately followed by a local minima in impedance for the group of electrodes near the temporal edge (*blue*) that lasted until approximately 140 weeks postoper-

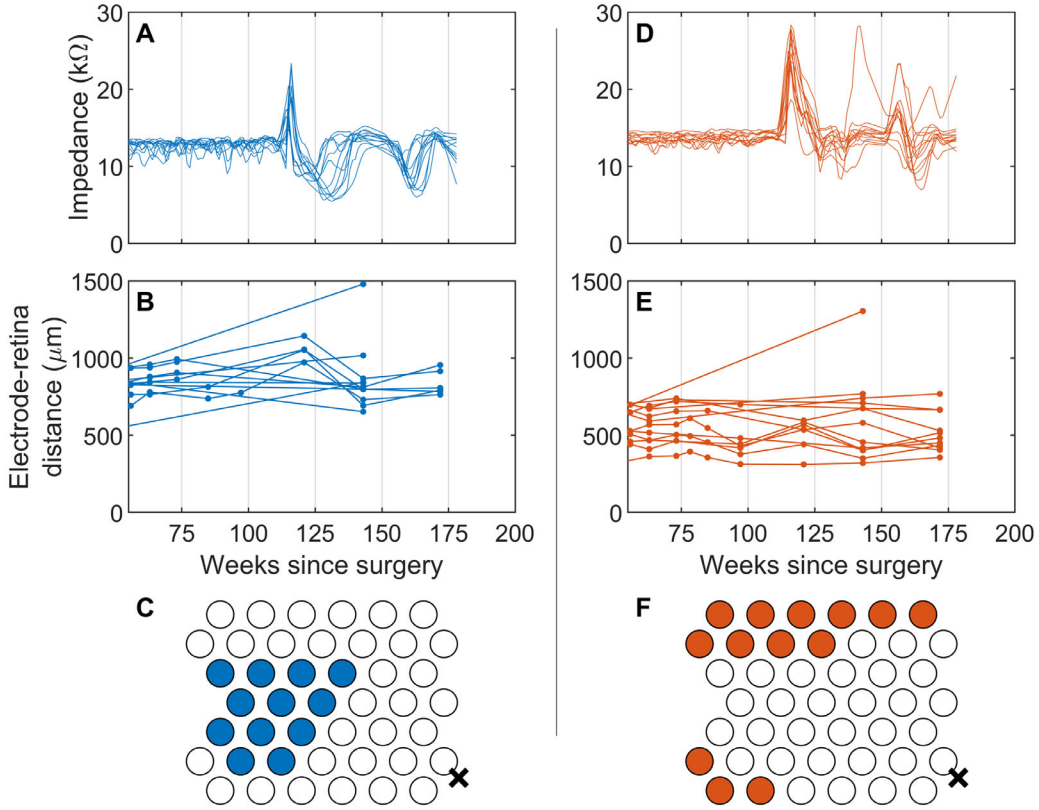

Figure 9. Changes in impedance that were apparently unrelated to stimulation were observed in S3 for a large number of electrodes between 115 and 140 weeks postoperatively. The affected electrodes are categorized into two distinct groups (*blue* and *red*) based on the shape of the impedance curve. (A) Longitudinal impedance measures for the first group of electrodes (*blue*). (B) Longitudinal electrode–retina distance measures for the first group of electrodes. (C) Schematic of the array showing the first group of electrodes highlighted in *blue*. The approximate location of the fovea is indicated by a *black cross*. (D) Longitudinal impedance measures for the second group of electrodes (*red*). (E) Longitudinal electrode–retina distance measures for the second group of electrodes. (F) Schematic showing the second group of electrodes highlighted in *red*. The approximate location of the fovea is indicated by a *black cross*. Impedance measures were smoothed using a median filter with a window width of 14 days. Note that these electrodes had been deactivated in the stimulation configuration deployed to the subject's device, and therefore received no stimulation except for impedance tests.

ative. Electrode–retina distances increased marginally during this time (Fig. 9B) before returning to previous values; however, electrode–retina distance measures are only available for a small subset of the affected electrodes during this period. The electrodes in both groups (*blue* and *red*) had been deactivated in the stimulation configuration deployed to the subject's device, and therefore received no stimulation during this period except for impedance tests. A second very similar spike in impedance followed by a local minima occurred between 155 and 170 weeks postoperatively, but OCT imaging was not acquired during this period owing to the COVID-19 pandemic. Electrode–retina distance measurements immediately around this event are limited to weeks 143 and 172. S3 reported spontaneous phosphenes (in absence of stimulation) twice during this period.

Discussion

This study reported observations regarding changes in the electrode-tissue interface during chronic stimulation with the second-generation (44-channel) suprachoroidal retinal prosthesis. Electrode impedances, electrode–retina distances, and perceptual thresholds were monitored in four recipients of the prosthesis over more than 154 weeks after implantation. During this time, the subjects used their prostheses in their daily lives and during regular training and assessments in the laboratory. For all subjects, electrode–retina distances increased in the months after implantation as expected from preclinical studies showing the development of a fibrotic capsule around the array.[13,14]

In three subjects, electrode–retina distances had plateaued by 15 months postoperative (45 weeks for S1, 63 weeks for S2, and 24 weeks for S3) and remained stable for the rest of the study. In the final subject, S4, the increase in electrode–retina distances remained statistically significant for the duration of the study, but the distance seems to be approaching an asymptote. At the study end point, the rate of increase for this subject was 0.33 microns per week, equivalent to just 17 microns per year if we assume a worst case constant rate (although the rate of increase seems to be decreasing over time, in congruence with the other subjects). This change is unlikely to be clinically significant and is approaching the limits of accuracy of OCT axial resolution (5 µm). Total charge delivered over the course of the study was smaller for S4 compared with the other subjects by more than six times, supporting the notion that the ongoing changes in the electrode–retina distance were unlikely to be stimulus related.

Perceptual thresholds decreased over time in subjects S1 and S3, which may suggest familiarization with the phosphenes or biological effects that were not detectable in this study. For subjects S2 and S4 perceptual thresholds increased slightly over the course of the study, although this effect was only statistically significant in S2. This could be explained by the fact that electrode-retina distances were slower to stabilize after surgery in S2 and S4 compared with S1 and S3, because an increased electrode–retina distance is expected to lead to increased perceptual thresholds.

In our previous trial of a prototype suprachoroidal retinal implant, electrode–retina distances trended upward over time.[10,11] It was hypothesized that high stimulation currents and pulse rates may have triggered inflammation or continued fibrotic growth, pushing the retina. Increasing electrode–retina distances led to increasing perceptual thresholds, requiring yet higher stimulation levels to evoke a percept, further compounding the effect. After further preclinical investigation[15] the charge density limits were revised for the second-generation prosthesis from 237 µC/cm^2 in the previous clinical trial to 32 µC/cm^2 for the present study. This change was achieved by increasing the electrode diameter (now ø1 mm compared with 0.6 mm and 0.4 mm) and decreasing the maximum allowable charge per phase. The maximum stimulation rate has also been decreased from 400 to 50 pulses per second. Our finding that electrode–retina distances and perceptual thresholds were stable supports the notion that chronic stimulation at these levels did not lead to changes in the electrode–tissue interface that adversely affected device function. Although enlarging the electrodes is generally expected to lead to a decreased spatial resolution, the second-generation device still provided significant improvement in visual function tasks (including a grating acuity task) and activities of daily living.[16–18]

This study is limited to four subjects with end-stage retinitis pigmentosa, observed over a maximum of 181 weeks postoperatively. Owing to limitations imposed by the COVID-19 pandemic, the follow-up period was different for each subject and there were sometimes long intervals between OCT data collection, which particularly limits our ability to detect short-term fluctuations in the electrode–retina distance. Use of the prosthesis in daily life was encouraged but not controlled. Habitual use patterns and the cumulative charge delivered over the study varied significantly between subjects.

Transient Impedance Changes

Although impedances were generally stable over time, transient changes in impedance lasting up to 40 weeks were observed in a small number of electrodes in subjects S2 and S3. In some cases, the change in impedance seemed to be stimulus related—a decrease in impedance corresponded closely with a period of high use of the affected electrodes, and impedances returned to normal values when stimulation ceased. The affected electrodes had relatively high charge requirements (perceptual thresholds), which is typical of peripherally located electrodes. The adjacent electrodes to the ones that displayed transient changes were not affected, and there was no detectable change in electrode–retina distances. We hypothesize that high levels of stimulation on the affected electrodes provoked a localized acute inflammatory response that decreased impedance. However, the inflammation must have been very minor and highly localized so as not to affect neighboring electrodes or cause a noticeable change in the electrode–retina distance. A change in stimulation parameters may be appropriate in cases where changes in impedance do not recover within a day.

Transient changes in impedance also occurred for electrodes covering a large area of the array in S3 between 115 and 140 weeks postoperative (Fig. 9). Initially, impedances increased abruptly and then quickly recovered. This was immediately followed by a temporary decrease in impedance for electrodes in a cluster near the temporal edge of the array, where the electrode–retina distances were greatest. It is unlikely that this change was in response to stimulation, because the affected electrodes received very little stimulation over the course of the study. The initial spike in impedance was greatest for electrodes along the superior edge of the array, and the leadwires

servicing those electrodes are bundled together and would experience similar mechanical forces. The subsequent local minima in impedance primarily affected electrodes near the temporal edge of the array, and we hypothesize this is due to an acute inflammatory response in the area. The patient reported spontaneous phosphenes (in absence of stimulation) twice during this period, which could have been triggered by mechanical pressure on the retina. Although it is generally expected that the implant is mechanically stable after the first few months after the surgery, we hypothesize that the observed short-term impedance changes were related to a mechanical perturbation of the implant, but the exact origins are unclear. Nevertheless, the participant continued to use the device at home without further issue.

Rapid Impedance Changes

We observed very short-term decreases in electrode impedances upon stimulation. Changes in impedance were observed after as little as 10 μC of charge (equivalent to just 0.8 s of stimulation at the safe charge limit of 250 nC per pulse and 50 pulses per second). When the cumulative charge delivered over the course of a day was in the order of millicoulombs, decreases in impedance as high as 60% were routinely observed. Impedances recovered to normal values during inactive periods, as evidenced by the fact that impedances measured before stimulation each day were stable longitudinally. Similar transient stimulus-induced reductions in impedance have been reported in cochlear implants. It is thought that a loss of protein cover over the electrode surface after stimulation leads to decreased polarization impedance, which then recovers during inactive periods as protein cover returns.[23,24]

Factors Affecting Perceptual Thresholds

Previous studies in suprachoroidal and epiretinal implants have reported a correlation between electrode–retina distance and perceptual thresholds.[6,7,9,10,25,26] In the present study, perceptual thresholds increased with electrode–retina distance in three of four subjects, but this effect was only statistically significant in one subject. The correlation between electrode–retina distance and thresholds may have been confounded by other factors. For example, thresholds are expected to be higher for electrodes in peripheral retinal locations, where density of retinal ganglion cells is lower and retinal degeneration in retinitis pigmentosa typically most advanced.

Conclusions

Device functionality remained within the predefined charge limits for all four subjects. Electrode impedances and electrode–retina distances were stable after an initial period of increase following implantation. Transient changes in impedance that seemed to be stimulus related were observed for a small number of electrodes in two subjects, but these changes resolved when stimulation ceased and did not result in any observable permanent physiological or perceptual changes. Chronic electrical stimulation with the 44-channel suprachoroidal retinal implant within a charge density limit of 32 $\mu C/cm^2$ per phase is suitable for long-term use in humans with retinitis pigmentosa.

Acknowledgments

The authors thank valuable assistance of Hannah Kamitakahara, Emma Perkins, and Aashraya Kumar.

Supported by the National Health and Medical Research Council (NHMRC) Grant 1082358 (P.J.A., M.P., L.A.; Canberra, ACT, Australia) and Bionic Vision Technologies Pty Ltd (Australia). The Bionics Institute and the Centre for Eye Research Australia wish to acknowledge the support of the Victorian Government through its Operational Infrastructure Support Program (Victoria, Australia), and the generous support of the estate of the late Brian Entwisle.

Disclosure: **S.A. Titchener**, Bionic Vision Technologies Pty Ltd (F); **D.A.X. Nayagam**, Bionic Vision Technologies Pty Ltd (F, P); **J. Kvansakul**, Bionic Vision Technologies Pty Ltd (F); **M. Kolic**, Bionic Vision Technologies Pty Ltd (F, R); **E.K. Baglin**, Bionic Vision Technologies Pty Ltd (F, R); **C.J. Abbott**, Bionic Vision Technologies Pty Ltd (R, F); **M.B. McGuinness**, None; **L.N. Ayton**, None; **C.D. Luu**, Bionic Vision Technologies Pty Ltd (F); **S. Greenstein**, None; **W.G. Kentler**, None; **M.N. Shivdasani,** None; **P.J. Allen,** Bionic Vision Technologies Pty Ltd (F, P); **M.A. Petoe,** Bionic Vision Technologies Pty Ltd (F, R, P)

References

1. Ayton LN, Barnes N, Dagnelie G, et al. An update on retinal prostheses. *Clin Neurophysiol*. 2019;131(6):1383–1398, doi:10.1016/j.clinph.2019.11.029.

2. Mirochnik RM, Pezaris JS. Contemporary approaches to visual prostheses. *Mil Med Res*. 2019;6(1):1.
3. Bloch E, Luo Y, da Cruz L. Advances in retinal prosthesis systems. *Ther Adv Ophthalmol*. 2019;11:2515841418817501, doi:10.1177/2515841418817501.
4. Cohen ED. Prosthetic interfaces with the visual system: biological issues. *J Neural Eng*. 2007;4(2):R14.
5. Shah S, Hines A, Zhou D, Greenberg RJ, Humayun MS, Weiland JD. Electrical properties of retinal–electrode interface. *J Neural Eng*. 2007;4(1):S24.
6. Mahadevappa M, Weiland JD, Yanai D, Fine I, Greenberg RJ, Humayun MS. Perceptual thresholds and electrode impedance in three retinal prosthesis subjects. *IEEE Trans Neural Syst Rehabil Eng*. 2005;13(2):201–206.
7. de Balthasar C, Patel S, Roy A, et al. Factors affecting perceptual thresholds in epiretinal prostheses. *Invest Ophthalmol Vis Sci*. 2008;49(6):2303–2314, doi:10.1167/iovs.07-0696.
8. Ahuja AK, Yeoh J, Dorn JD, et al. Factors affecting perceptual threshold in Argus II retinal prosthesis subjects. *Transl Vis Sci Technol*. 2013;2(4):1, doi:10.1167/tvst.2.4.1.
9. Xu LT, Rachitskaya A V, DeBenedictis MJ, Bena J, Morrison S, Yuan A. Correlation between Argus II array–retina distance and electrical thresholds of stimulation is improved by measuring the entire array. *Eur J Ophthalmol*. 2021;31(1):194–203, doi:10.1177/1120672119885799.
10. Shivdasani MN, Sinclair NC, Dimitrov PN, et al. Factors Affecting Perceptual Thresholds in a Suprachoroidal Retinal Prosthesis. *Invest Ophthalmol Vis Sci*. 2014;55(10):6467–6481, doi:10.1167/iovs.14-14396.
11. Ayton LN, Blamey PJ, Guymer RH, et al. First-in-human trial of a novel suprachoroidal retinal prosthesis. *PLoS One*. 2014;9(12):e115239.
12. Sinclair NC, Shivdasani MN, Perera T, et al. The appearance of phosphenes elicited using a suprachoroidal retinal prosthesis. *Invest Ophthalmol Vis Sci*. 2016;57(11):4948–4961, doi:10.1167/iovs.15-18991.
13. Abbott CJ, Nayagam DAX, Luu CD, et al. Safety studies for a 44-channel suprachoroidal retinal prosthesis: a chronic passive study. *Invest Ophthalmol Vis Sci*. 2018;59(3):1410–1424, doi:10.1167/iovs.17-23086.
14. Nayagam DAX, Williams RA, Allen PJ, et al. Chronic electrical stimulation with a suprachoroidal retinal prosthesis: a preclinical safety and efficacy study. *PLoS One*. 2014;9(5):e97182.
15. Nayagam DAX, Thien PC, Abbott CJ, et al. A preclinical model for safe retinal stimulation. *Invest Ophthalmol Vis Sci*. 2017;58(8):4204.
16. Petoe MA, Titchener SA, Kolic M, et al. A second-generation (44-channel) suprachoroidal retinal prosthesis: interim clinical trial results. *Transl Vis Sci Technol*. 2021;10(10):12, doi:10.1167/tvst.10.10.12.
17. Karapanos L, Abbott CJ, Ayton LN, et al. Functional vision in the real-world environment with a 44-channel suprachoroidal retinal prosthesis. *Invest Ophthalmol Vis Sci*. 2021;62(8):3203.
18. Titchener SA, Kvansakul J, Shivdasani MN, et al. Oculomotor responses to dynamic stimuli in a 44-channel suprachoroidal retinal prosthesis. *Transl Vis Sci Technol*. 2020;9(13):31.
19. Saunders AL, Williams CE, Heriot W, et al. Development of a surgical procedure for implantation of a prototype suprachoroidal retinal prosthesis. *Clin Exp Ophthalmol*. 2014;42(7):665–674.
20. Drasdo N, Fowler CW. Non-linear projection of the retinal image in a wide-angle schematic eye. *Br J Ophthalmol*. 1974;58(8):709.
21. Dacey DM, Petersen MR. Dendritic field size and morphology of midget and parasol ganglion cells of the human retina. *Proc Natl Acad Sci U S A*. 1992;89(20):9666–9670.
22. Baglin EK, Kolic M, Titchener SA, et al. A 44 channel suprachoroidal retinal prosthesis: inter-observer reliability measuring electrode to retina distance. *Invest Ophthalmol Vis Sci*. 2019;60(9):4991.
23. Newbold C, Mergen S, Richardson R, et al. Impedance changes in chronically implanted and stimulated cochlear implant electrodes. *Cochlear Implants Int*. 2014;15(4):191–199.
24. Newbold C, Richardson R, Millard R, Seligman P, Cowan R, Shepherd R. Electrical stimulation causes rapid changes in electrode impedance of cell-covered electrodes. *J Neural Eng*. 2011;8(3):36029.
25. Kasi H, Hasenkamp W, Cosendai G, Bertsch A, Renaud P. Simulation of epiretinal prostheses—evaluation of geometrical factors affecting stimulation thresholds. *J Neuroeng Rehabil*. 2011;8(1):1–10.
26. McMahon MJ, Fine I, Greenwald SH, et al. Electrode impedance as a predictor of electrode–retina proximity and perceptual threshold in a retinal prosthesis. *Invest Ophthalmol Vis Sci*. 2006;47(13):3184.